

Dynamics of snakes and ladders

Keith A. May

McGill Vision Research Unit, Department of Ophthalmology,
McGill University, Montréal, Québec, Canada



Robert F. Hess

McGill Vision Research Unit, Department of Ophthalmology,
McGill University, Montréal, Québec, Canada



D. J. Field, A. Hayes, and R. F. Hess (1993) introduced two types of stimulus to study the perceptual integration of contours. Both types of stimulus consist of a smooth path of spatially separate elements, embedded in a field of randomly oriented elements. In one type of stimulus (“snakes”), the elements form tangents to the path of the contour; in the other type (“ladders”), the elements are orthogonal to the path. Little is currently known about the relative integration speeds of these two types of contour. We investigated this issue by temporally modulating the orientations of the contour elements. Our results suggest that snakes and ladders are integrated at similar speeds.

Keywords: contour integration, temporal, speed, snakes, ladders

Citation: May, K. A., & Hess, R. F. (2007). Dynamics of snakes and ladders. *Journal of Vision*, 7(12):13, 1–9, <http://journalofvision.org/7/12/13/>, doi:10.1167/7.12.13.

Introduction

One of the oldest unsolved problems in vision science is the question of how the visual system groups spatially separate elements of a display to form a coherent whole. An early exposition of this problem was provided by Ehrenfels (1890/1988). Ehrenfels’s student, Wertheimer (1923/1938), formulated a set of “Laws of Organization,” now known as the *Gestalt laws*, to describe various grouping phenomena.

The Gestalt laws amounted to observations of grouping phenomena but gave little insight into the underlying mechanisms. To achieve a better understanding of visual grouping, Field, Hayes, and Hess (1993) introduced a new type of stimulus to investigate the grouping of elements along a contour. The target contour consisted of spatially separate elements positioned along a smooth path. The contour was embedded in a field of randomly oriented distractor elements with the same spatiotemporal properties as the contour elements. The spatial separation of the distractors was approximately matched to the separation of the contour elements, so that the contour could only be distinguished from the background by virtue of the fact that the contour elements formed a smooth path.

Most studies of contour integration have used contours in which the elements formed tangents to the path. However, a few studies have shown that it is possible to detect contours in which the elements are perpendicular to the path. These two types of contour were labeled “snakes” and “ladders,” respectively, by Bex, Simmers, and Dakin (2001). Ladders are generally harder to detect than snakes (Bex et al., 2001; Field et al., 1993; Hess, Ledgeway, & Dakin, 2000; Ledgeway, Hess, & Geisler, 2005) but are much easier to

detect than contours in which the elements are oriented at 45° to the path (Ledgeway et al., 2005).

There are several different methods by which contour integration could be achieved (Watt, Dakin, & Ledgeway, *in press*). These include association field mechanisms (e.g., Field et al., 1993), Delaunay triangulation (e.g., Watt et al., *in press*), and algorithms based on spatial overlap of filter responses (e.g., Hess & Dakin, 1997). It may be that snake and ladder contours are both integrated using the same kind of mechanism. Ledgeway et al. (2005) argued in favor of this view and sketched out an association field model in which there were strong connections between collinear elements and weak connections between parallel elements. May and Hess (*in press*) implemented a model of this kind, in which snake associations were about twice as strong as ladder associations. In constructing their model, May & Hess borrowed a key feature from Pelli, Palomares, and Majaj’s (2004) model of crowding: The minimum association field size at each point in the visual field was proportional to the eccentricity. This feature allowed May and Hess’s model to explain a striking difference between snakes and ladders: Straight snakes are easily detectable far into the periphery, whereas straight ladders are undetectable at quite small eccentricities.

An alternative view is that snakes and ladders are detected by completely different mechanisms. For example, snakes might be detected using an association field mechanism, whereas ladders might be detected by looking for extended regions of response in the output of a second-order channel, such as those proposed in many models of texture segregation (Graham, 1991; Graham & Sutter, 1998; Graham, Beck, & Sutter, 1992; Graham, Sutter, & Venkatesan, 1993; Lin & Wilson, 1996; Sutter, Beck, & Graham, 1989; Wilson, 1993).

To derive a realistic model of how the human visual system integrates snake and ladder contours, it is essential that we learn as much as possible about the similarities and differences between the mechanisms that detect these two types of contour. To this end, our study compared the integration speeds of snake and ladder contours. Highly curved contours are integrated more slowly than straight ones (Hess, Beaudot, & Mullen, 2001), but little else is known about the speed of contour integration.

Recently, Cass and Spehar (2005a, 2005b) investigated the cortical propagation speed of the facilitation signals underlying the flanker facilitation effect. They argued that the facilitation signal was faster when the target and the flankers were parallel (as in the ladder contour configuration) than when they were collinear (snake configuration). This does not necessarily imply a similar difference in the integration speed of snake and ladder contours because it is unlikely that contour integration and flanker facilitation are mediated by the same mechanisms (Huang, Hess, & Dakin, 2006; Williams & Hess, 1998). However, the fact that snake and ladder configurations showed differences in the speed of one type of contextual influence suggested that it might be fruitful to investigate the speed of another type of contextual influence, namely, contour integration.

Methods

We measured contour integration speed using a similar method to Hess et al. (2001), in which the orientations of the individual elements were flipped between the snake (or ladder) configuration and a masking configuration in which each element was oriented obliquely relative to the contour. We varied the temporal frequency of the orientation flipping, by varying the duration for which the elements were held constant at each orientation, and found the duration corresponding to threshold performance. We reasoned that a shorter duration threshold would correspond to a higher integration speed because, with a shorter duration, the integration process would need to be faster to integrate the contour before the interruption occurred. It appears that contour integration mechanisms have a limited ability to integrate across multiple exposures: Hess et al.

found that multiple exposures gave similar duration thresholds to single exposures, in which the target stimulus was temporally sandwiched between two masking stimuli. The advantage of multiple exposures is that it equalizes the total amount exposure to the stimulus and therefore equalizes the effect of any lapses of attention: For single exposures, a momentary lapse of attention might have a worse effect on short durations than long durations, which could cause the integration time to be overestimated.

One potential difficulty in comparing the propagation speed of the two contour types is that, with stationary stimuli, performance on ladders is usually inferior to snakes (Bex et al., 2001; Field et al., 1993; Ledgeaway et al., 2005). If ladders were closer to threshold than snakes without orientation flipping, then, as the image duration was reduced in the orientation-flipping conditions, ladders might reach threshold sooner than snakes, even if the integration signal was generally no slower for ladders. To avoid this problem, the difficulty levels of stationary snakes and ladders were equalized to a performance level of around 85% correct by jittering the orientations of the elements relative to the path (in Experiment 1) or by varying in the path angle (i.e., curvature) of the contour (in Experiment 2). Thus, both types of contour were at the same (below ceiling) performance level without temporal modulation, so we could fairly compare the effect of temporal modulation on the two contour types.

We ran separate pilot experiments for each subject to find the jitter levels (in Experiment 1) or path angles (in Experiment 2) corresponding to 85% correct. In these pilot experiments, we found the percent correct at a range of levels of orientation jitter (or path angle), fitted a psychometric function to the data, and used this psychometric function to determine the level corresponding to 85% correct. The jitter levels used in Experiment 1 are given in Table 1, and the path angles used in Experiment 2 are given in Table 2.

Subjects

Three subjects participated in Experiment 1: two male observers (KAM and BCH) and one female observer (PCH). KAM and BCH had participated in several

Subject	Snake jitter level		Ladder jitter level	
	Separation 1.54°	Separation 3.08°	Separation 1.54°	Separation 3.08°
BCH	21.5	16.2	18.7	15.7
PCH	18.1	17.7	13.2	4.81
KAM (0° path angle)	19.4	18.3	18.1	13.5
KAM (20° path angle)	17.0	12.5	12.8	2.21

Table 1. Orientation jitter levels for each subject, contour type, and element separation in Experiment 1. These values give the standard deviation (in degrees) of the Gaussian distribution from which the jitter value was selected on each trial. The values were determined from a pilot experiment and corresponded to the jitter levels that would give rise to a performance of 85% correct in the unmasked (1,067 ms image duration) condition of Experiment 1.

	Separation 1.54°	Separation 3.08°
Snake	32.1	21.7
Ladder	20.6	14.2

Table 2. Path angles for each contour type and element separation in [Experiment 2](#). These values were determined from a pilot experiment and corresponded to the path angles that would give rise to a performance of 85% correct in the unmasked (1,067 ms image duration) condition of [Experiment 2](#).

previous experiments on contour integration and had equal experience on snakes and ladders. PCH had participated in previous experiments on contour integration but was relatively inexperienced at detecting ladders. KAM and PCH had corrected-to-normal vision; BCH had 20/20 vision without correction. BCH and PCH were naive to the purposes of the experiment. Only KAM participated in [Experiment 2](#).

Apparatus

The experiments were run on a Dell PC with a VSG 2/5 graphics card (Cambridge Research Systems, Rochester, UK). Experiments were controlled using software written in MATLAB (The MathWorks, Inc.). Images were generated using C routines called from MATLAB. The images were linearly scaled to fit the range 0–255 and stored in an 8-bit frame store on the VSG card. Stimuli were then scaled to the correct contrast and were gamma corrected by mapping the 8-bit values onto 15-bit values. An analogue input to the monitor was generated from these 15-bit values using two 8-bit digital-to-analogue converters in the VSG card. Stimuli were displayed on a Sony G520 monitor at a frame rate of 120 Hz. The graphics card was configured to generate a screen display that measured 1,024 pixels horizontally by 769 pixels vertically. Subjects viewed the screen binocularly from a distance of 60 cm.

Stimuli

On each trial, one interval contained a stimulus consisting of a path of odd-symmetric Gabor elements embedded in a grid of similar Gabor distractors; the other interval contained a stimulus consisting only of distractors. The Gabor elements were generated using [Equation 1](#):

$$L(x, y) = L_0(1 + cw), \quad (1)$$

where c is the carrier and w is the envelope, as defined in [Equations 2](#) and [3](#), respectively,

$$c = C \sin[2\pi f(x \cos \theta + y \sin \theta)], \quad (2)$$

$$w = \exp\left(\frac{-(x^2 + y^2)}{2\sigma^2}\right). \quad (3)$$

L is the luminance at position (x, y) , measured from the center of the Gabor patch; L_0 is the mean (background) luminance of 52 cd/m²; C is the Michelson contrast, which was set to 0.9; f is the spatial frequency of the Gabor carrier, which was 5.19 cycles/deg; σ controls the “width” of the Gaussian envelope and was set to 0.136 degrees of visual angle; θ is the orientation of the element from vertical.

Stimuli were generated using a similar procedure to that of Beaudot and Mullen (2003). The stimulus area was divided into an invisible 10 × 10 square grid. For stimuli containing no contour, each grid square was filled with one randomly oriented Gabor element, placed at a random location within the square, subject to the constraint that the elements should not overlap too much. For stimuli containing a contour, the contour was first positioned randomly within the grid, and then each remaining empty grid square was filled with one element with random orientation and random position within the grid square.

Part of a snake contour is represented schematically in [Figure 1](#). The contour was constructed along an invisible backbone of 10 line segments, joined end-to-end. A contour element was placed at the center of each segment. The distance between adjacent elements along the contour is referred to as the element separation, s . Both experiments used two different element separations (1.54° and 3.08° visual angle). For snake contours, the element was oriented parallel to the segment; for ladders, the element was orthogonal to the segment. In [Experiment 1](#), having selected the element orientation according to the contour type (snake or ladder), the orientation was then jittered by

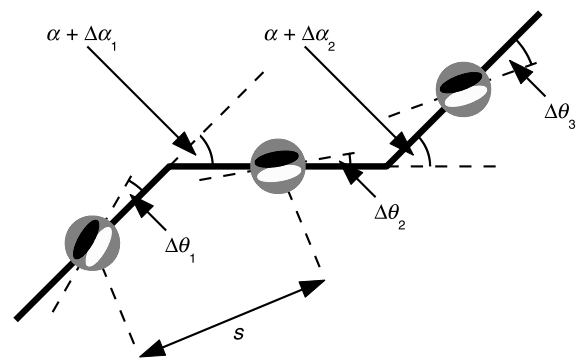


Figure 1. A schematic representation of part of a snake contour, illustrating the different parameters. The thick solid lines represent the invisible segments that form the backbone of the contour. A Gabor element was positioned at the midpoint of each segment. For snakes, each element, i , was aligned with its segment before a jitter value, $\Delta\theta_i$, was added to its orientation. For ladders, the element was orthogonal to its segment before adding the jitter value. There was no orientation jitter in [Experiment 2](#). s is the element separation, that is, the distance between adjacent elements along the contour. The angle between each segment, i , and the next was equal to $\pm\alpha$ (the path angle) plus a random jitter value, $\Delta\alpha_i$. The sign of the path angle was randomly determined for each junction between segments.

adding a random value selected from a Gaussian probability distribution. The standard deviations of these distributions for each condition and each subject are given in [Table 1](#). There was no orientation jitter in [Experiment 2](#).

The absolute difference in orientation between adjacent segments is referred to as the path angle. The sign of this difference was random for each pair of adjacent segments. For each pair, the path angle was jittered by adding a random value uniformly distributed between $\pm 10^\circ$.

[Table 3](#) gives a summary of all the stimulus parameters. The width of the grid squares was set to $2s/(1 + \sqrt{2})$, which ensured that the mean separation between adjacent distractors was close to the element separation, s (Beaudot & Mullen, 2003). For more details of the contour generation algorithm, see Beaudot and Mullen (2003).

For each stimulus, there was a corresponding mask which was identical to the stimulus, except that the orientation of each element was rotated by 45° . Adjacent elements along the contour always rotated in different directions; the direction of rotation of distractor elements was random.

Examples of the stimuli are shown in [Figure 2](#). There were two intervals of 1,067 ms, each preceded by a fixation dot with duration 1,067 ms. The stimuli in the two intervals were generated using the same stimulus parameters, except that one stimulus contained a snake or a ladder contour and the other had no contour. During each 1,067 ms interval, the display alternated between stimulus and mask, each displayed for the same fixed duration, which we call the image duration. The image duration took values of 16.67, 33.33, 66.67, 133.3, 266.7, 533.3, and 1,067 ms (these durations corresponded to 2, 4, 8, 16,

32, 64, and 128 frames of the CRT display). The stimulus always came before the mask in the sequence. For the highest image duration, only the stimulus could be presented within the 1,067 ms allocated to the interval, so this condition was effectively unmasked, containing a stationary stimulus. The temporal properties of this condition were identical to the pilot experiments, which found the orientation jitter levels ([Experiment 1](#)) or path angles ([Experiment 2](#)) corresponding to 85% correct.

Procedure

In [Experiment 1](#), the trials were blocked according to contour type (snake or ladder) and element separation (1.54° or 3.08° visual angle). For subjects BCH and PCH, all the paths were straight, that is, the path angle was 0° (except for a small random jitter). KAM performed the same conditions as the other subjects, plus an additional set of blocks in which the path angle was 20° . Within a block of trials, there were 20 trials for each image duration, randomly distributed within the block. There were five blocks for each combination of contour type and element separation, giving 100 trials per condition. Each trial consisted of two temporal intervals, one containing a contour stimulus (as in [Figure 2a](#) or [2b](#)) and the other containing a no-contour stimulus ([Figure 2c](#)). During the interval, the display alternated between stimulus and mask. Subjects had to indicate, with a button press, which interval contained the contour. Auditory feedback was given. All stimuli within a block had the same orientation jitter level, which was set according to the values given in [Table 1](#), to achieve a performance level of 85% correct in the unmasked (1,067 ms image duration) condition.

[Experiment 2](#) was very similar to [Experiment 1](#). As before, the trials were blocked according to contour type and element separation, and within each block, there were 20 trials for each image duration. The only differences were that, in [Experiment 2](#), there was no orientation jitter, and the path angle within each block was set according to the values given in [Table 2](#) to achieve a performance level of 85% correct in the unmasked (1,067 ms image duration) condition. Only KAM participated as a subject in [Experiment 2](#).

Results

Experiment 1

The performance on each condition of [Experiment 1](#) is shown in [Figure 3](#). For each contour type, we fitted a cumulative Gaussian psychometric function to the data, using *psignifit* (<http://www.bootstrap-software.org/psignifit/>),

Parameter	Value
Michelson contrast	0.9
Carrier spatial frequency (cycles/deg)	5.19
Carrier wavelength, λ (degrees of visual angle)	0.193
σ (degrees of visual angle)	0.136
λ/σ	$\sqrt{2}$
Separation, s (degrees of visual angle)	1.54, 3.08
s/λ	8, 16
s/σ	11.3, 22.6
Path angle	Experiment 1 : 0° (all subjects), 20° (KAM only); Experiment 2 : see Table 2
Path angle jitter	Uniform probability between $\pm 10^\circ$
Orientation jitter	Experiment 1 : see Table 1 ; Experiment 2 : none
Stimulus duration	1,067 ms
Interstimulus interval duration	1,067 ms

Table 3. Stimulus parameters.

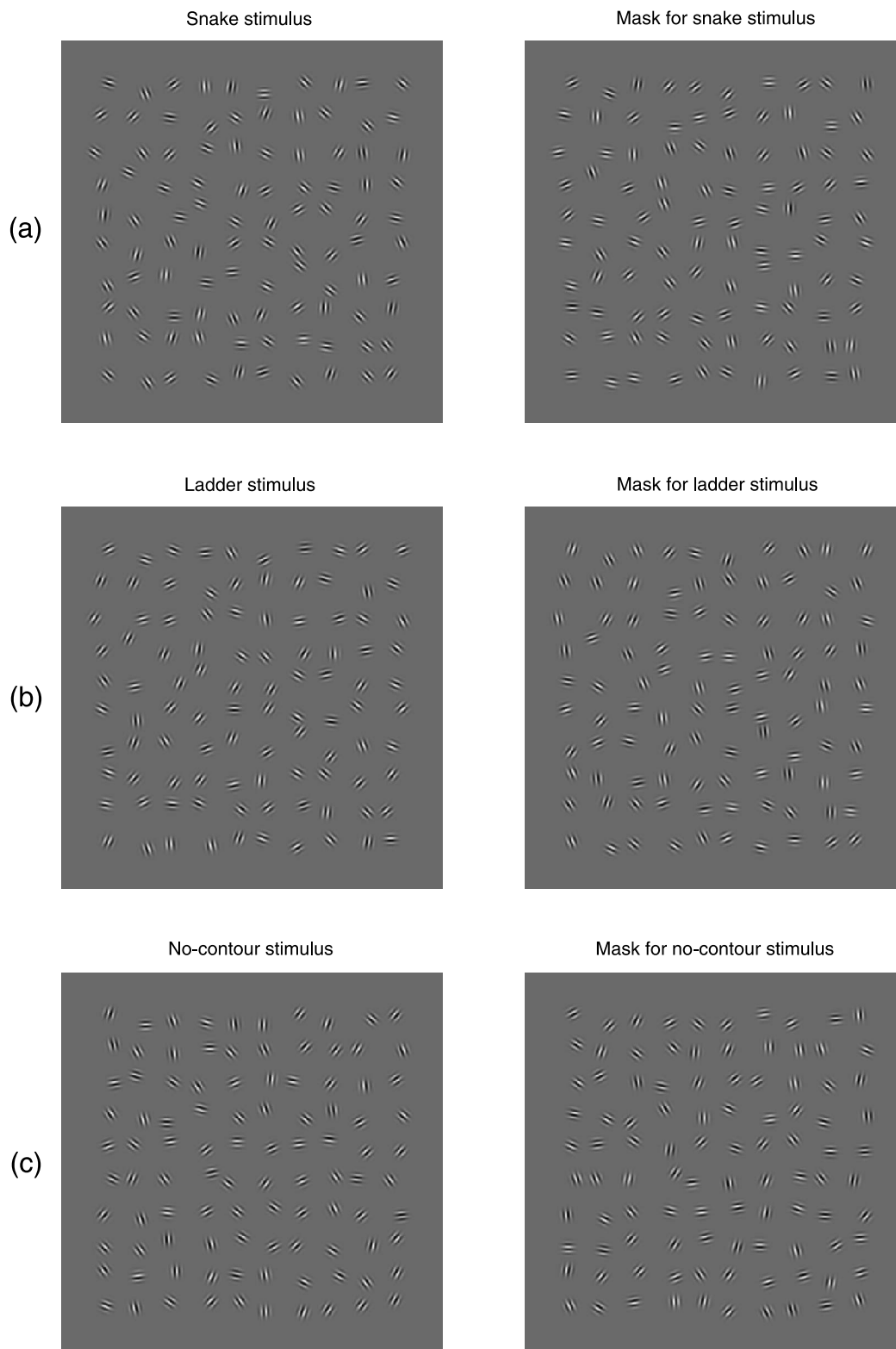


Figure 2. Examples of the stimuli and corresponding masks from the 0° path angle condition in [Experiment 1](#). The deviations from straightness in the contours are caused by the path angle jitter. To make the contours in this figure more visible, no orientation jitter was used. Readers who have difficulty seeing the contours can view [supplementary Figure S1](#), in which the contour elements have a higher contrast than the distractor elements. (a) A snake stimulus and corresponding mask; (b) a ladder stimulus and mask with elements positioned in the same locations as for the snake stimulus; (c) no-contour stimulus and mask. During each 1,067 ms interval, the display alternated between stimulus and mask. One interval in each trial contained a contour stimulus (snake or ladder) and the other contained a no-contour stimulus. Each interval was preceded by a fixation dot for 1,067 ms.

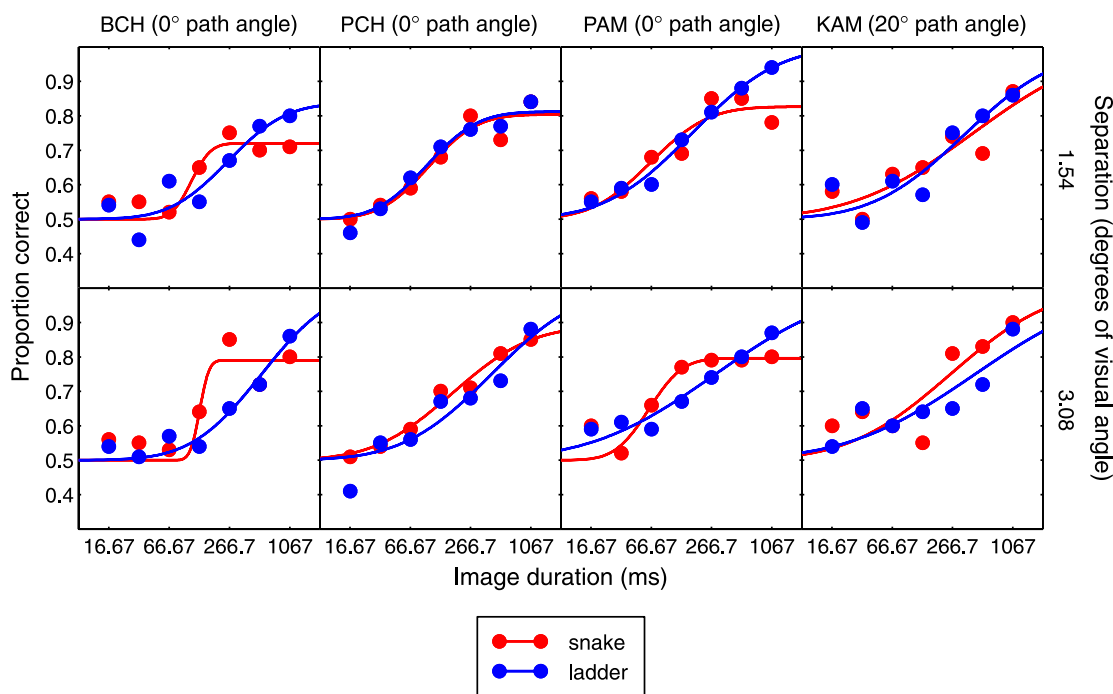


Figure 3. Raw data from Experiment 1, with best-fitting cumulative Gaussian functions.

a software package that implements the maximum likelihood method described by Wichmann and Hill (2001a). The psychometric functions had the following form:

$$y = 0.5 + (0.5 - \lambda)F(x; \alpha, \beta), \tag{4}$$

where x is the logarithm of the image duration, y is the performance level (proportion correct), and F is the integral of a unit-area Gaussian with position α and standard derivation β . The value of λ (which determines the maximum value of the function) was unconstrained.

The fitted psychometric functions are shown in Figure 3. Functions for snakes and ladders were very similar. This was quantified by finding the duration threshold corresponding to a performance level of 67.5% correct, which was halfway between chance and 85% correct (85% correct is the performance level that we aimed to achieve, by means of orientation jitter, in the 1,067 ms condition). Figure 4 shows that the image duration thresholds were very similar for snakes and ladders. There was a slight trend for snakes to have lower thresholds, but none of the differences were statistically reliable: The bootstrap error bars always overlapped.

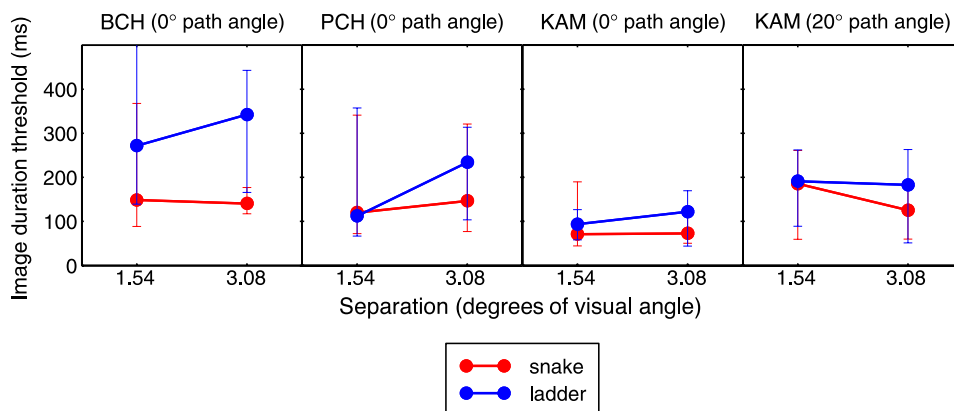


Figure 4. Image duration thresholds corresponding to a performance level of 67.5% correct in Experiment 1. These thresholds were determined from the psychometric functions shown in Figure 3. The error bars show 5% and 95% confidence limits. These were found using the percentile bootstrap method implemented by *psignifit* (see Wichmann & Hill, 2001b); each confidence limit was based on 10,000 Monte Carlo simulations.

The auxiliary file “Expt_1_data.txt” contains the raw data, the parameters of the psychometric functions, and the thresholds and confidence limits.

Experiment 2

The data were analyzed in the same way as in [Experiment 1](#). [Figure 5](#) shows the raw data and the psychometric functions, and [Figure 6](#) shows the image duration thresholds corresponding to 67.5% correct. Thresholds for snakes and ladders were extremely similar. The auxiliary file “Expt_2_data.txt” contains the raw data, the parameters of the psychometric functions, and the thresholds and confidence limits.

Discussion

In every condition of our experiments, threshold performance levels on snakes and ladders corresponded to similar image durations, suggesting that these two types of contour are integrated at similar speeds.

A possible criticism of our experimental design is that, to equalize performance on snakes and ladders in the unmasked (1,067 ms) condition, we introduced a confounding variable of orientation jitter ([Experiment 1](#)) or

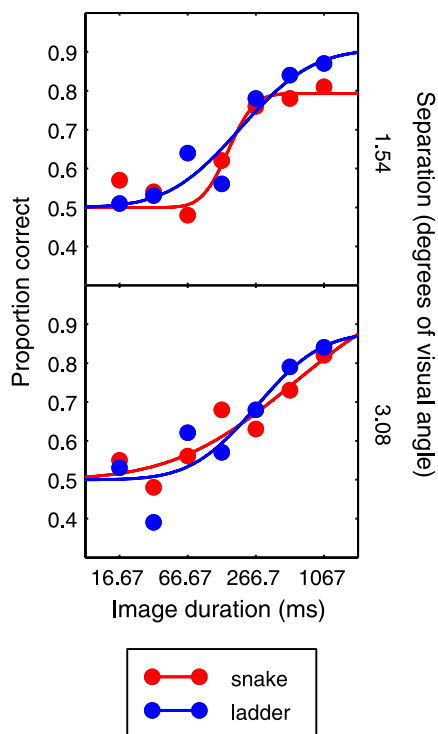


Figure 5. Raw data from [Experiment 2](#), with best-fitting cumulative Gaussian functions.

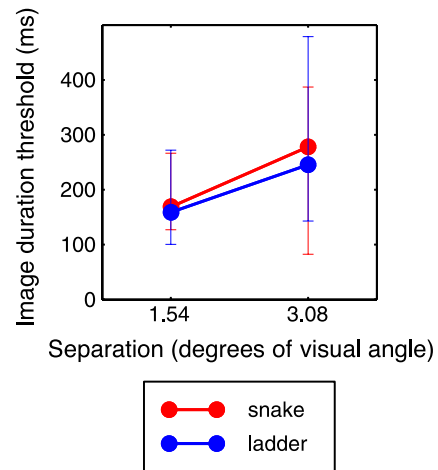


Figure 6. Image duration thresholds corresponding to a performance level of 67.5% correct in [Experiment 2](#). These thresholds were determined from the psychometric functions shown in [Figure 5](#). The error bars show 5% and 95% confidence limits, determined as in [Figure 4](#).

path angle ([Experiment 2](#)). The effect of orientation jitter on integration time has not been investigated, but the available evidence on the effect of path angle suggests that increasing the path angle would increase the integration time (Hess et al., 2001), and it is possible that orientation jitter would have a similar effect. However, [Table 1](#) shows that, for some conditions, the orientation jitter levels were very similar for snakes and ladders; the fact that, even on these conditions, we failed to find a difference between snakes and ladders suggests that these two types of contour are indeed integrated at similar speeds.

It is interesting to compare our results with those of Cass and Spehar (2005a, 2005b). They argued that, in the flanker facilitation effect, the facilitation signal propagates across the cortex more quickly for the ladder configuration than the snake configuration. Our finding that snake and ladder contours are integrated at the same speed might therefore be seen as further evidence against the hypothesis that flanker facilitation and contour integration are mediated by the same mechanisms. However, this argument is fairly weak because our methods differed substantially from those of Cass and Spehar. In fact, Cass and Spehar’s results may have nothing to do with propagation speed. They varied the target–flanker separation and, for each separation, found the shortest stimulus duration for which flanker facilitation was found. They found that this critical duration increased with separation, with a sharper increase for the snake configuration. This was interpreted as indicating that the facilitatory signal takes longer to propagate across the cortex for snakes. However, an alternative interpretation is that the critical duration reflects the strength of the facilitatory connection. In this case, if the strength of the facilitatory connection dropped off sharply with distance for snakes, but more

gradually for ladders, then we would predict that the critical duration would vary with distance more sharply for snakes, thus explaining Cass and Spehar's results without any reference to differences in propagation speed. We thank Li Zhaoping (personal communication) for this suggestion. This alternative interpretation does not apply to our study because we measured integration time by varying temporal, not spatial, properties of the stimuli.

Conclusions

Our results suggest that snake and ladder contours are integrated at similar speeds. Contour integration may therefore have different temporal dynamics to flanker facilitation, for which it has been claimed that the ladder configuration is processed more quickly (Cass & Spehar, 2005a, 2005b). Our findings are consistent with the idea that snakes and ladders are integrated using the same kind of mechanism (Ledgeway et al., 2005; May & Hess, [in press](#)).

Acknowledgments

This work was supported by CIHR grant MT 108-18 to Robert F. Hess.

Commercial relationships: none.

Corresponding author: Keith A. May.

Email: keith@keithmay.org.

Address: Vision Sciences Research Group, School of Life Sciences, University of Bradford, Richmond Road, Bradford, West Yorkshire, BD7 1DP, UK.

References

- Beaudot, W. H. & Mullen, K. T. (2003). How long range is contour integration in human color vision? *Visual Neuroscience*, *20*, 51–64. [[PubMed](#)]
- Bex, P. J., Simmers, A. J., & Dakin, S. C. (2001). Snakes and ladders: The role of temporal modulation in visual contour integration. *Vision Research*, *41*, 3775–3782. [[PubMed](#)]
- Cass, J. R., & Spehar, B. (2005a). Dynamics of collinear contrast facilitation are consistent with long-range horizontal striate transmission. *Vision Research*, *45*, 2728–2739. [[PubMed](#)]
- Cass, J. R., & Spehar, B. (2005b). Dynamics of cross- and iso-surround facilitation suggest distinct mechanisms. *Vision Research*, *45*, 3060–3073. [[PubMed](#)]
- Ehrenfels, C. (1988). Über 'Gestaltqualitäten'. *Vierteljahrsschrift für Wissenschaftliche Philosophie* (vol. 14, pp. 242–292). In B. Smith (Ed. & Trans.), *Foundations of Gestalt Theory* (pp. 82–117). Munich & Vienna: Philosophia. (Original work published 1890).
- Field, D. J., Hayes, A., & Hess, R. F. (1993). Contour integration by the human visual system: Evidence for a local "association field." *Vision Research*, *33*, 173–193. [[PubMed](#)]
- Graham, N. (1991). Complex channels, early local nonlinearities, and normalization in texture segregation. In M. Landy & J. A. Movshon (Eds.), *Computational models of visual processing* (pp. 273–290). Cambridge, MA: MIT Press.
- Graham, N., Beck, J., & Sutter, A. (1992). Nonlinear processes in spatial-frequency channel models of perceived texture segregation: Effects of sign and amount of contrast. *Vision Research*, *32*, 719–743. [[PubMed](#)]
- Graham, N., & Sutter, A. (1998). Spatial summation in simple (Fourier) and complex (non-Fourier) texture channels. *Vision Research*, *38*, 231–257. [[PubMed](#)]
- Graham, N., Sutter, A., & Venkatesan, C. (1993). Spatial-frequency- and orientation-selectivity of simple and complex channels in region segregation. *Vision Research*, *33*, 1893–1911. [[PubMed](#)]
- Hess, R. F., Beaudot, W. H., & Mullen, K. T. (2001). Dynamics of contour integration. *Vision Research*, *41*, 1023–1037. [[PubMed](#)]
- Hess, R. F., & Dakin, S. C. (1997). Absence of contour linking in peripheral vision. *Nature*, *390*, 602–604. [[PubMed](#)]
- Hess, R. F., Ledgeway, T., & Dakin, S. C. (2000). Impoverished second-order input to global linking in human vision. *Vision Research*, *40*, 3309–3318. [[PubMed](#)]
- Huang, P. C., Hess, R. F., & Dakin, S. C. (2006). Flank facilitation and contour integration: Different sites. *Vision Research*, *46*, 3699–3706. [[PubMed](#)]
- Ledgeway, T., Hess, R. F., & Geisler, W. S. (2005). Grouping local orientation and direction signals to extract spatial contours: Empirical tests of "association field" models of contour integration. *Vision Research*, *45*, 2511–2522. [[PubMed](#)]
- Lin, L. M., & Wilson, H. R. (1996). Fourier and non-Fourier pattern discrimination compared. *Vision Research*, *36*, 1907–1918. [[PubMed](#)]
- May, K. A., & Hess, R. F. (in press). Ladder contours are undetectable in the periphery: A crowding effect?
- Pelli, D. G., Palomares, M., & Majaj, N. J. (2004). Crowding is unlike ordinary masking: Distinguishing feature integration from detection. *Journal of Vision*, *4*(12):12, 1136–1169, <http://journalofvision.org/4/12/12/>, doi:10.1167/4.12.12. [[PubMed](#)] [[Article](#)]
- Sutter, A., Beck, J., & Graham, N. (1989). Contrast and spatial variables in texture segregation: Testing a

- simple spatial-frequency channels model. *Perception & Psychophysics*, *46*, 312–332. [[PubMed](#)]
- Watt, R. J., Dakin, S. C., & Ledgeway, T. (in press). Families of models for the Gabor path paradigm.
- Wertheimer, M. (1938). Untersuchungen zur Lehre von der Gestalt II. *Psychologische Forschung* (vol. 4, pp. 301–350). In Ellis, W. (Trans.), *A source book of gestalt psychology* (pp. 71–88). London: Routledge & Kegan Paul. (Original work published 1923).
- Wichmann, F. A., & Hill, N. J. (2001a). The psychometric function: I. Fitting, sampling, and goodness of fit. *Perception & Psychophysics*, *63*, 1293–1313. [[PubMed](#)] [[Article](#)]
- Wichmann, F. A., & Hill, N. J. (2001b). The psychometric function: II. Bootstrap-based confidence intervals and sampling. *Perception & Psychophysics*, *63*, 1314–1329. [[PubMed](#)] [[Article](#)]
- Williams, C. B., & Hess, R. F. (1998). Relationship between facilitation at threshold and suprathreshold contour integration. *Journal of the Optical Society of America A, Optics, image science, and vision*, *15*, 2046–2051. [[PubMed](#)]
- Wilson, H. R. (1993). Nonlinear processes in visual pattern discrimination. *Proceedings of the National Academy of Sciences of the United States of America*, *90*, 9785–9790. [[PubMed](#)] [[Article](#)]